Automated Segmentation and Hybrid Classifier for Identifying Medical Image

Tak-Yee Wong[2] and Ching-Hsue Cheng[1*]

[1]*Department of Information Management, National Yunlin University of Science and Technology, 123, Section 3, University Road, Touliu, Yunlin 640, Taiwan*
[2]*Department of Radiology, St. Martin de Porres Hospital, Chiai Taiwan*
chcheng@yuntech.edu.tw

Abstract

The high prevalence of lung cancer, many researcher concerns about diagnosing pulmonary lesions in chest computed tomography (CT). However, specialists would spend a great amount of their time and effort to analysis those CT scans. And the inter-reader variability in the detection of nodules by specialists may exist. Therefore, many automated methods have proposed methods for automatic diagnosis to assist artificial inspection. This study proposes a novel hybrid method to initially classify lungs images. Firstly, adjusting the contrast of chest images can change those images from indistinct to clear, and then use the proposed novel hybrid method to automated identification CT images. From the experiments, this paper can obtain three contributions: (1) Proposed segmentation algorithm can refine the lungs regions and improve the classification performance. (2) The proposed method can be executed before doctor diagnosis or computer-aided system, which can be sure that input CT image need to be detected out the actual positions, shapes or other information of nodules. (3) The results display a higher accuracy in proposed rough classifier based on DWPT-SVD than other classification methods, which verifies that proposed method can reduce time and cost of lung nodule diagnosis.

Keywords: *Computed tomography, Segmentation algorithm, Singular value decomposition (SVD), Discrete wavelet packets transform (DWPT)*

1. Introduction

In recent years, lung cancer has been attracting the attention of medical and scientific ranges because of its high prevalence related with the difficult treatment. From 2008 the statistics indicate that lung cancer of the globe is the one which attacks the greatest number of people. If the lung cancer can be identified in initial stages, the patient's 5-year survival probability just raise up to 70% [1], the previous diagnosis is the best way to treat successfully.

Chest computed tomography (CT) is a well-established tool, which help for diagnosing pulmonary metastasis in tumor patients, even assist in evaluating lung disease progression and regression during the treatment period. CT techniques have been utilized to screening lung cancer in high-risk individuals and are very useful for identifying early lung cancer [2] and the inter-reader variability in the detection of nodules by specialists may exist [3]. Therefore, there are many computational methods proposed for aiding doctor diagnosis in order to improve the existing mechanisms. The existing systems which their structures include a classification component have demonstrated better performances than their counterparts [4].

In addition, there are many published papers automatically detecting lung nodule by tracing lungs contour and scanning nodule contour or shape microscopically. As Yeny and Helen (2008) [5] used scan line search for smoothing lung boundary. Dehmeshki, *et al.*, [6] separate

nodules from adjoining blood vessels by calculating 3D geometric feature and volumetric shape index of each voxel. Mullaly, *et al.*, [7] utilizes nodule size, location, shape and exclusivity measures to matching nodules.

According to foregoing papers, an intelligent detection system would have a large amount of computing processes. But pay attention to a key point, if those all lungs images must be detected? Even though a patient has trouble with pulmonary nodule positively, which can't sure every one slice of his chest CT scan has nodules. If input the all of scans, which wastes a great amount of processing time. There is other choice, before starting to nodule detection system, let specialists recognize all input data whether it has nodule and whether it needs to be detected by auto diagnosis systems. While the choice is adopted, there is an interesting thought, why not the specialists directly inspect those chest CT images? There are equal time would be spent.

Hence, this study proposes the three stages automated pulmonary segmentation algorithm (AS algorithm) and the classification nodule method through Rough Set (RS) based on DWPT-SVD (Discrete wavelet packets transform- Singular Value Decomposition). First, the lungs which are the region of Interest (ROI) were extracted from chest CT image with three stages automated segmentation algorithm. The performance of proposed segmentation method will be compared with a region growing method. Then, the DWPT-SVD was applied to obtain characteristic values of pulmonary images. Finally, those characteristic values were utilized as attributes for RS to classify pulmonary images.

This paper proposes automated pulmonary segmentation algorithm (AS method) and the classification nodule method through Rough Set (RS) based on DWPT-SVD is proposed in this study. First, the lungs which are the region of Interest (ROI) were extracted from chest CT image with three stages automated segmentation algorithm. The performance of proposed segmentation method will be compared with a region growing method. Then, the DWPT-SVD was applied to obtain characteristic values of pulmonary images. Finally, those characteristic values were utilized as attributes for RS to classify pulmonary images.

2. Related Works

This section introduces some important literatures, which includes SVD, DWPT, and RS.

2.1 Singular Value Decomposition

Singular Value Decomposition (SVD) [8] is a matrix factorization technique. Suppose that the input image is represented by a matrix A. For convenience, assume that A is an M×N matrix with rank r. The SVD of A can be represented, as in (1).

$$\mathrm{SVD}(A) = U \times D \times V^T \qquad (1)$$

$$\mathrm{A} = UDV^T = \begin{bmatrix} u_{1,1} & \cdots & u_{1,M} \\ u_{2,1} & \cdots & u_{2,M} \\ \vdots & \ddots & \vdots \\ u_{M,1} & \cdots & u_{M,M} \end{bmatrix} \begin{bmatrix} d_1 & 0 & \cdots & 0 \\ 0 & d_2 & \cdots & 0 \\ \vdots & \vdots & \ddots & \vdots \\ 0 & 0 & \cdots & d_r \end{bmatrix} \begin{bmatrix} v_{1,1} & \cdots & v_{1,N} \\ v_{2,1} & \cdots & v_{2,N} \\ \vdots & \ddots & \vdots \\ v_{N,1} & \cdots & v_{N,N} \end{bmatrix}^T$$

U and V are orthogonal matrices with dimensions $M \times M$ and $N \times N$, respectively. D, called the singular matrix, is an $M \times N$ diagonal matrix whose diagonal entries are non-negative real numbers.The initial r diagonal entries of $D(d_1, d_2, \cdots, d_r)$ have the property that $d_i > 0$ and $d_1 \geq d_2 \geq \cdots \geq d_r$.

SVD can provide the best low-rank approximation of the original matrix, A, which is an attribute particularly useful in the case of Recommender Systems. By retaining the first $k \ll r$ singular values of D and discarding the rest, which, based on the fact that the entries in D are sorted, can be translated as keeping the k largest singular values, we reduce the dimensionality of the data representation and hope to capture the important "latent" relations existing but not evident in the original representation of matrix A. The resulting diagonal matrix is termed D^k. Matrices U and V should be also reduced accordingly. U_k is produced by removing $r - k$ columns from matrix U. V_k is produced by removing $r - k$ rows from matrix V. Matrix A_k is defined as (2).

$$A_k = U_k \times D_k \times V_k^T \quad (2)$$

A_k represents the closest linear approximation of the original matrix A with reduced rank k. Once this transformation is completed, users and items can be thought off as points in the k-dimensional space [9].

2.2 Discrete Wavelet Packets Transform

Nowadays, wavelet transforms rapidly surface in various regions as telecommunications, radar target recognition, and texture image classification [10]. The main advantage of wavelets is that they have a varied window size, which can be wide for slow frequencies and narrow for the fast ones, thus results in optimal time–frequency resolution in all frequency ranges [11]. Furthermore, owing to the fact that windows are adapted to the transients of each scale, wavelets lack the requirement of stationary [12, 13].

In the tradition, discrete wavelet transform only recursively decompose the low frequency band, but some high-frequencies are worth to decompose for getting more information. Discrete wavelet packet analysis is an extension of the discrete wavelet transform, and discrete wavelet packet transform (DWPT) allows both detail and approximation result to be decomposed further, which can use a low pass filters collection and high-pass filters collection to decompose coefficient of detail result (as Figure 1 and Figure 2). The Figure 1, L-L1 is approximation and others are details. In other words, the Figure 2, L-L2 is approximation and others are details. Thus, the detail sub-bands can be further decomposed.

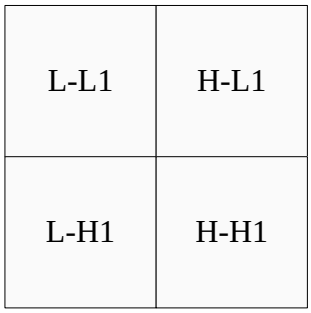

Figure 1. 1-level WPDT

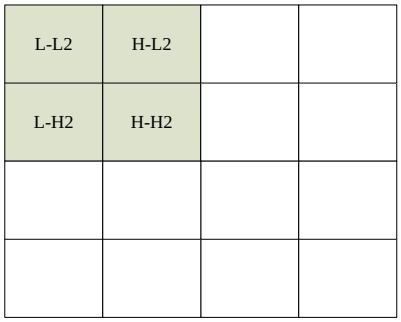

Figure 2. 2-level WPDT

The advantage of wavelet packet analysis is that it can possibly combine the different levels of decomposition in order to achieve the optimum time–frequency representation of the original [14]. The standard 2D-DWPT can be implemented with a low-pass filter h and a high-pass filter g [15]. The 2D-DWPT of an $N \times M$ discrete image X up to level $p + 1$

$\left(p \le min(\log_2 N, \log_2 M)\right)$ is recursively defined in terms of the coefficients at level as equation(3):

$$C_{4k,(i,j)}^{p+1} = \sum_m \sum_n h(m)h(n)C_{k,(m+2i,n+2j)}^{p}$$
$$C_{4k+1,(i,j)}^{p+1} = \sum_m \sum_n h(m)\mathrm{g}(n)C_{k,(m+2i,n+2j)}^{p}$$
$$C_{4k+2,(i,j)}^{p+1} = \sum_m \sum_n \mathrm{g}(m)h(n)C_{k,(m+2i,n+2j)}^{p}$$
$$C_{4k+3,(i,j)}^{p+1} = \sum_m \sum_n \mathrm{g}(m)\mathrm{g}(n)C_{k,(m+2i,n+2j)}^{p} \qquad (3)$$

Where $C_{0,(i,j)}^{0}$ is the image$X$. At each step, the image C_k^p is decomposed into four quarter-size images $C_{4k}^{p+1}, C_{4k+1}^{p+1}, C_{4k+2}^{p+1}, C_{4k+3}^{p+1}$ as shown in Figure 3 and Figure 4.

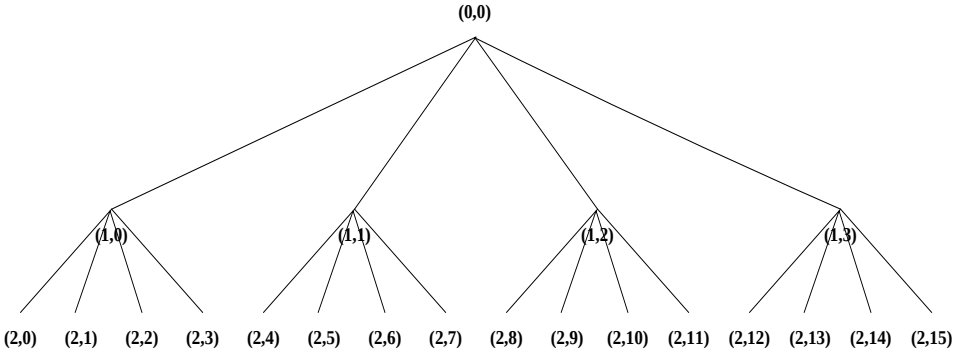

Figure 3. 2-level Wavelet Packet Decomposition Tree

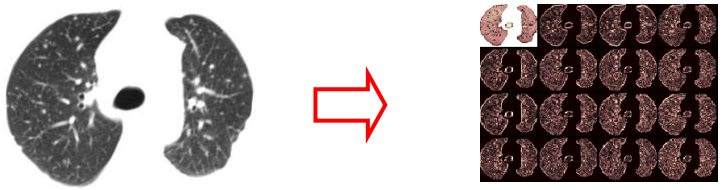

(a) the original lungs image (b)project onto each leaf node of the tree

Figure 4. The Original Image Presented on left is Decomposed at 2-level DWPT

2.3 Rough Sets Theory

Pawlak (1982) [16] proposed the rough sets theory in 1982 for distilling the rules to support making decision. This theory can be seen as a new mathematical approach to vagueness [17]. The mathematical basis of rough set theory just is the indiscernibility relation [17]. Attribute reduction is an important issue in the Rough Sets Theory, a good reduction where the reduced set of attributes can provide the same quality of approximation as the original set of attributes.

The philosophy of rough set is founded on the assumption that with every object of the universe of discourse associated some information (data, knowledge). For example, while

objects are representation of patients with certain disease, the information just is the symptoms of the disease. Some objects characterized by the same information, which are indiscernible because of their similarity in view of the available information about them. The mathematical basis of rough set theory just is the indiscernibility relation [16].

Rough sets have two precise sets, called the lower and the upper approximation [16, 17]. The lower one means all objects in this approximation which surely belong to the set, and the upper approximation consists of all objects possibly belonging to the set. The difference between the upper and the lower approximation composes the boundary region of the rough sets. Figure 5 shows the basic notions in rough sets.

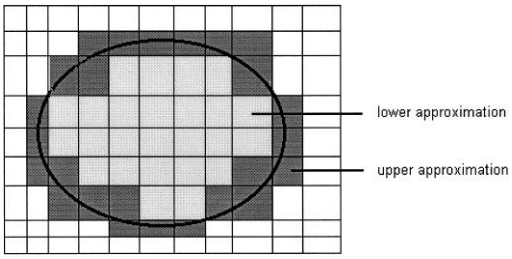

Figure 5. Basic Notions of Rough Sets

Attribute reduction is an important issue in the Rough Sets Theory, a good reduction where the reduced set of attributes can provide the same quality of approximation as the original set of attributes. Using an attributes reduction technique, the rules could be found by determining the decision attributes value based on condition attributes values. Therefore, the rules are presented in an "IF condition(s) THEN decision(s)" format. The concept of decision table is employed in this study, to establish rules from fuzzy relationships. Which generates rule for better forecasting results.

Rough sets have some of advantages in the following:

(1) Rough sets do not require any preliminary or additional parameter about data (i.e. rough sets are application processing easily).

(2) Rough sets can deal with complex information, and gain simple and rules of Knowledge.

(3) Rough sets can delete the redundant of attributes and find the small subsets in which we are interested.

(4) Rough sets offer the ability to handle large amounts of both quantitative and qualitative data and it is not necessary that the variables employed satisfy any assumption.

(5) Using rough sets to analyze results, the rules are easily understandable and easily interpretable.

3. Proposed Method

Respecting the time-consuming of nodule detection no matter for specialists and previous related systems are described as in Section 1, presenting a pre-classification mechanism before those systems begin to detect nodule microscopically. To ensure the input image has nodule indeed, so it must be recognized carefully. Thus it can improve the existing mechanism of lung disease diagnosis for doctor and computer-aided systems. This paper proposed a

novel hybrid method of lung nodule classification based on DWPT-SVD, *i.e.*, use SVD to improve its performance.

For easy computation and understanding, an algorithm was proposed. Before introducing the algorithm, the experimental data sets are simply described in advance. The experimental chest CT images have 100 chest CT images of size 512 × 512 from Lung Image Database Consortium (LIDC). Randomly sample 75 images as training data, the remained 25 lungs images are regarded as testing data. The testing data is randomly selected non-overlapping the same as training data.

The proposed algorithm contains 7 main steps specified as follows: (1) adjust image contrast, (2) Lung extraction, (3) SVD image reconstruction, (4) compute DWPT feature extraction, (5) compute feature value and reduce attribute, and (6) classify lungs images. Each step is described in detail as follows:

Step1: Adjust Image Contrast

Firstly, the LIDC original image (as Figure 6) was adjusted automatically by Adjust Contrast Tool (see Figure 7), and then its histogram of intensities as shown in Figure 8. In chest CT images, there are two principal regions with different density distribution: (1) the low-density region, which includes the background air, lungs and bronchial tree, and (2) the high-density region, which contains the fat, muscles and bones.

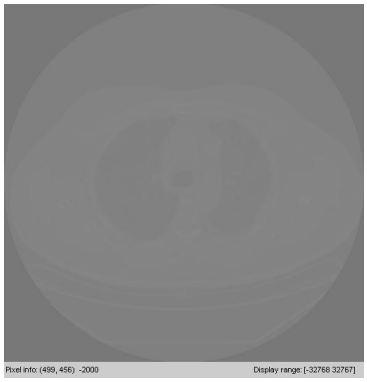

Figure 6. The Original Chest Image

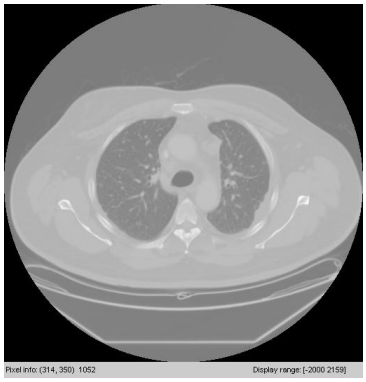

Figure 7. The Image Adjusted First

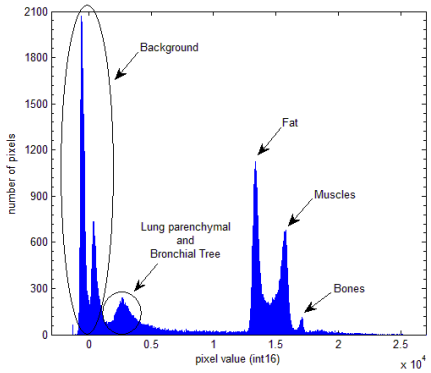

Figure 8. The Histogram of Image Intensities

Second, the image (Figure 7) adjusted automatically was adjusted the contrast again, display range of the image was set in the start point of background and the end point of before

fat. And then the range selected was expanded into whole pixels range (as Figure 9). (The whole range of type int16 is from -32,768 to 32,767). At last, the result as show in Figure 10, the high-density region, which meanings the fat, muscles and bones, became in one density (white), since these high-density region were excluded from display range.

Then, the result image can be processed in next step, Lung Extraction.

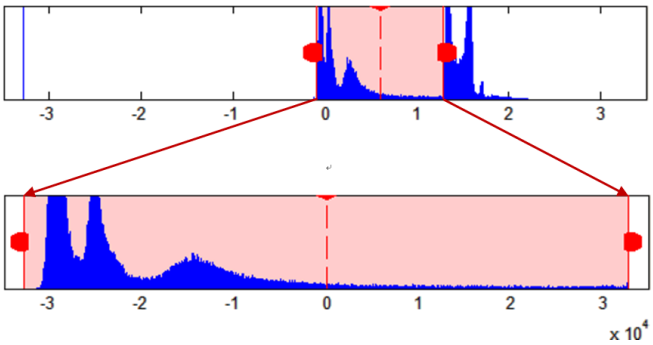

Figure 9. The Range Selected was Expanded into Whole Pixels Range

Figure 6. The Adjusted Result Image

Step 2: Lung Extraction

In order to refine the region of interesting (ROI) in proposed algorithm for accurate experimental results, the lungs were extracted from chest CT images. The proposed automated segmentation (AS) algorithm are (a) segmenting roughly chest, (b) filling the background, and (c) extracting the bounding box of lungs. The more explanation is introduced in the following.

(a) Segmenting Roughly Chest

From the image can see the lungs regions are all white, their values are 1. Begin to roughly segment chest, the input image is scanned for every rows and columns from four directions. Scan every column from image left and from right, and then scan every row from top and from the bottom of image. During the scan process, the sum of pixel values of each row and each column was calculated. And then assign a threshold value, if the sum of a row or column is bigger than threshold, the row or column was recorded. Because of the chest region pixel value is 1 (white), if scan line enter the chest region, the sum would be bigger than back-

ground region. Finally, chest region was segmented roughly according to those rows and columns positions.

(b) Filling the Background

This step fills the background from dark to white. The scan line will check each pixel value, if the value is smaller than 1, the value could be reset to 1. The scan line would stop when it enter the chest region, which has the more white pixels. A threshold would be set, if the checking pixel value is 1, then suppose it's some following pixel values all are 1, the threshold just is the sum of their values. Afterward, if the real sum is smaller than the threshold, which indicates the pixels are not all white, and then continues to scan and reset. Contrariwise, if all the pixels are white, which represents the scan line is enter the chest, so it can stop scanning.

(c) Extracting the Bounding Box of Lungs

After the step two, the region besides the lungs was filled with white. In this final step, the bounding box of lungs would be extracted. The scan line is also used in this stage, and the operation is likely to stage two. Scan line would check each pixel for one line, if the pixel value is not 1 that means the scan line enter the lung, the position of scan line was recorded. Finally like the stage one, the positions information of the four direction scan line was used to segment the bounding box of lungs. At last, the result of region growing method is illustrated in "Figure 11". And the result of proposed AS algorithm is shown on "Figure 12.".

Step 3: Reconstruct SVD Image

The SVD can compute the matrix singular value decomposition of image or signal.[8] This step uses SVD to execute the decomposition of lungs images, and then rebuilds images by those matrices calculated from SVD method. Given the input lungs image which size of 512 × 512 , singular value decomposition (SVD) can decompose A into A = UDVT where U and V are square matrices (512 × 512) and D is a singular, diagonal matrix. The numbers in the diagonal line of D matrix are singular values of the image A. If values locate the more upper left side, the more important characteristics of image. "Figure 13." shows the portion of singular values of image A. If values locate the more upper left side, the more important characteristics of image.

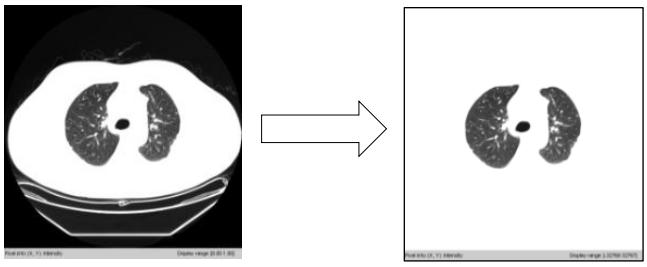

Figure 11. The Result of Region Growing Method

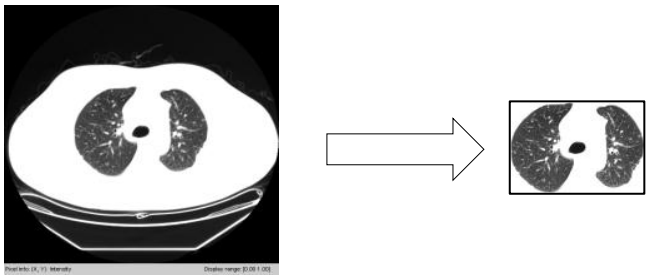

Figure 12. The Result of Proposed AS Algorithm

30523.19	0	0	0	0	0	0	0	0
0	3978.234	0	0	0	0	0	0	0
0	0	2048.307	0	0	0	0	0	0
0	0	0	1081.304	0	0	0	0	0
0	0	0	0	995.6717	0	0	0	0
0	0	0	0	0	719.8778	0	0	0
0	0	0	0	0	0	627.9078	0	0
0	0	0	0	0	0	0	563.7742	0
0	0	0	0	0	0	0	0	480.3623

Figure 13. The Singular Values of Image *A*

Then chooses singular values in order to reconstruct image. The more number of singular values is used, the image is more distinct. The meaning is that image reconstructed will be more similar to original input image A. In this study the all singular values are chose into rebuild work. Figure14 shows that the reconstruction images by SVD with 10, 20, 30, and all of the singular values. We can see that the more number of singular values is used, the image is clearer.

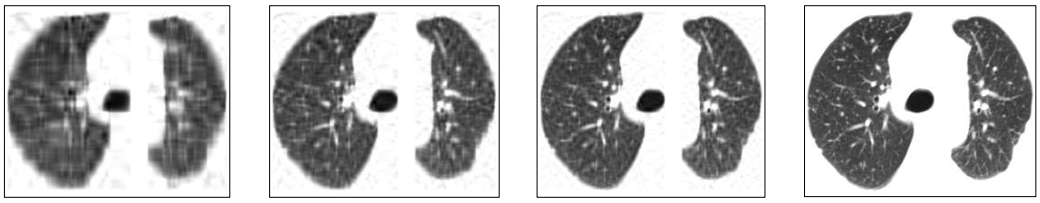

(a) (b) (c) (d)

Figure 14. The Reconstruction Images: (a) 10 (b) 20 (c) 30 (d) all of the Singular Values

Step 4: Compute DWPT feature extraction

This phase is responsible to DWPT-SVD system for extracting feature from lungs images. The feature extraction process has two sub-steps:

(1)Wavelet packet decomposition

For wavelet decomposition of lungs images, the pyramid structure of multi-resolution was used at depth m = 1 and m = 2. While m = 1, there are total 4 DWPT coefficients (1 approximate and 3 detail coefficients as "Figure 15(a)") calculated for each of these image regions. If m = 2, total 16 DWPT coefficients (1 approximate and 15 detail coefficients as "Figure 15(b)") are calculated for each of these image regions. Therefore, DWPT coefficients are sum of 20. In this study, wavelet packet decomposition was applied to the lungs images using Bi-or2.2 wavelet filters.

(2)Wavelet packet entropy

Entropy is a common thought which is applicable to many ranges, especially in image processing and signal processing. For each of those DWPT coefficients, the wavelet packet norm entropy values are computed by equation (4) as follows:

$$\text{Norm entropy} = \frac{1}{N}\sum_{i,j=1}^{N}|t(i,j)|^{p} \qquad (4)$$

(a) (b)

Figure 15. (a) The 4 DWPT Coefficients, and (b) the 16 DWPT Coefficients for Lungs Images

Where p is the power and its range must be such that $1 \leqq p < 2$, N is size of lungs images, t(i, j) is the transformed value in (i, j) for any sub-band (one of L-Li, L-Hi, H-Li, and H-Hi) of size N × N [18] The norm entropy of the lungs images was calculated as defined in equation (4) at the terminal node acquired from wavelet packet decomposition. This study sets p = 1.

Step 5: Compute Feature Value and Reduce Feature

This step concerns computing wavelet packet feature values of eight branch datasets, just like Step 4. According to Avei's method [11], which use the statistical values as input values, in this study, the similar statistical values are adopted to compute the features, which are mean value, median value, mode value, maximum value, minimum value, range value, standard deviation, median absolute value, and mean absolute value.

This paper uses reduct sets of rough sets to select wavelet packet feature values, the reduct sets is shown in Table 1. From the last column of Table 1, the intersection of all reducts is empty. Therefore, the dataset can't find the core set, *i.e.*, this step can't reduce any feature, and then the main features are range value, mean value, minimum value, maximum value, standard deviation and mean absolute value.

Step 6: Classify Lungs Images

This step realizes the intelligent classifier by LEM2 algorithm [19] of rough sets. From Step 5, the dataset of 6 main features values and one class feature was fed into rough sets system, then generated classification rules and got the results of classifying the images by

those classification rules. The LIDC datasets were classified into three classes: nodule, non-nodule and inflammation.

Table 1. Reduct Wavelet Packet Feature Value of one Dataset without SVD

(1-6)	Size	Pos.Reg.	SC	Reducts
1	1	1	1	{range}
2	1	1	1	{mean}
3	1	1	1	{min}
4	1	1	1	{max}
5	1	1	1	{standard-deviation}
6	1	1	1	{mean-absolute-deviation }

4. Experimental and Results

This section illustrates the experiment process for the proposed method. The LIDC data have been collected from five different sites in the United States [20]. The format of LIDC dataset is DICOM, it has high resolution and sensitivity for anatomy of chest. The LIDC dataset has 100 chest CT images. Randomly sample 75 images as training data, the remained 25 lungs images are regarded as testing data. The testing data is randomly selected non-overlapping the same as training data.

Then the LIDC dataset is verified by the proposed method, and compares proposed automated segmentation algorithm with region growing. The experiment results are shown in Table 2. The first columns of Table 2 show the results which used proposed method to classify test data. In addition to compare the datasets, the differences of proposed segmentation algorithm and region growing method will be discussed. Furthermore, the proposed DWPT-SVD method also will be compared with DWPT.

Table 2. Proposed Methods and Other Methods Results of LIDC

Methods		**Proposed**	**Trees.J48**	**Naïve Bayes**	**Multilayer Perception**	**SMO**
Region growing	DWPT	96.80% (0.031)	78.50% (12.98)	79.70% (12.18)	80.00% (9.95)	77.40% (9.91)
	DWPT-SVD	97.80% (0.038)	79.40% (11.53)	80.10% (12.35)	79.80% (9.95)	77.40% (10.21)
Proposed segmentation algorithm	DWPT	99.17% (0.026)	86.90% (9.40)	82.10% (11.83)	84.70% (11.59)	80.90% (10.55)
	DWPT-SVD	99.41% (0.018)	87.42% (9.68)	83.18% (10.51)	84.48% (11.16)	81.13% (10.91)

Note: The accuracy is average of 10 experiments and standard deviation is put in bracket.

The rest columns of Table 2 further display the other methods on the dataset: Trees J48, Naïve Bayes, Multilayer Perception, and SMO. There will be more discoveries. The accuracy is the average of 10 experiments for each part, and the standard deviation of the times is recorded. Table 2 shows that the other four classifiers are not greater than proposed method, and their stability also is not excellent.

5. Conclusions

This paper has proposed a novel hybrid method to initially classify lungs images. From the result, the proposed segmentation algorithm obviously can improve the performance. The accuracy can reach to 99.17% and 99.41% in third column of Table 2, those are higher than the accuracy of region growing method in all 5 classifiers. And the standard deviation of accuracy, the proposed segmentation algorithm has more stability (smaller). Then we can see that the proposed method, the accuracy shown SVD image reconstruction can raise the performance of classification. Table 2 also can discover that the four compared classifier are not greater than proposed method.

References

[1] J. R. Sousa, A. C. Silva, A.C. de Paiva and R. A. Nunes, "Methodology for automatic detection of lung nodules in computerized tomography images", Computer Methods and Programs in Biomedicine, vol. 98, **(2010)**, pp. 1-14.
[2] H. Helen, L. Jeongjin and Y. Yeny, "Automatic lung nodule matching on sequential CT images", Computers in Biology and Medicine, vol. 38, **(2008)**, pp. 623-634.
[3] S. G. Armato, G. McLennan, M. F. McNitt-Gray, C. R. Meyer, D. Yankelevitz, D. R. Aberle and L. P. Clarke, "Lung image database consortium developing a resource for the medical imaging research community", Radiology, vol. 232, **(2004)**, pp. 739-748.
[4] S. L. A. Lee, A. Z. Kouzani and E. J. Hu, "Random forest based lung nodule classification aided by clustering", Computerized Medical Imaging and Graphics, vol. 34, **(2010)**, pp. 535-542.
[5] Y. Yeny and H. Helen, "Correction of segmented lung boundary for inclusion of pleural nodules and pulmonary vessels in chest CT images", Computers in Biology and Medicine, vol. 38, **(2008)**, pp. 845-857.
[6] J. Dehmeshki, X. Ye, X. Y. Lin, M. Valdivieso and H. Amin, "Automated detection of lung nodules in CT images using shape-based genetic algorithm", Computerized Medical Imaging and Graphics, vol. 31, **(2007)**, pp. 408-417.
[7] W. Mullaly, M. Betke, H. Hong, J. Wang, K. Mann and J. P. Ko, "Multi-criterion 3D segmentation and registration of pulmonary nodules on CT: a preliminary investigation", Proceedings of the International Conference on Diagnostic Imaging and Analysis (ICDIA), **(2002)**, pp. 176-181.
[8] M. G. Vozalis and K. G. Margaritis, "Using SVD and demographic data for the enhancement of generalized Collaborative Filtering", Information sciences, vol. 177, **(2007)**, pp. 3017-3037.
[9] K. L. Chung, W. N. Yang, Y. H. Huang, S. T. Wu and Y. C. Hsu, "On SVD-based watermarking algorithm", Applied Mathematics and Computation, vol. 188, **(2007)**, pp. 54-57.
[10] E. Avci, "An expert system based on Wavelet Neural Network-Adaptive Norm Entropy for scale invariant texture classification", Expert Systems with Applications, vol. 32, **(2007)**, pp. 919-926.
[11] E. Avci, "Comparison of wavelet families for texture classification by using wavelet packet entropy adaptive network based fuzzy inference system", Applied Soft Computing, vol. 8, **(2008)**, pp. 225-231.
[12] E. Avci, I. Turkoglu and M. Poyraz, "A new approach based on scalogram for automatic target recognition with X-band Doppler radar", Asian Journal of Information Technology, vol. 4, **(2005a)**, pp. 133-140.
[13] E. Avci, I. Turkoglu and M. Poyraz, "Intelligent target recognition based on wavelet packet neural network", Expert Systems with Applications, vol. 29, **(2005b)**, pp. 175-182.
[14] S. Mallat and S. Zhong, "Characterization of signals from multiscale edges", IEEE Transactions Pattern Analysis and Machine Intelligence, vol. 14, **(1992)**, pp. 710-732.
[15] S. Mallat, "A Wavelet Tour of Signal Processing", Academic Press. New York: Academic Press, **(1999)**.
[16] Z. Pawlak, "Rough sets", International Journal of Computational Information Science, **(1982)**, pp. 341-356.
[17] Z. Pawlak and A. Skowron, "Rudiments of rough sets", Information Sciences, vol. 177, **(2007)**, pp. 3-27.
[18] S. Arivazhagan and L. Ganesan, "Texture classification using wavelet transform", Pattern Recognition Letters, vol. 4, **(2003)**, pp. 1513-1521.
[19] J. W. Grzymala-Busse, "A new version of the rule induction system LERS", Fundamenta Informaticae, vol. 31, **(1997)**, pp. 27-39.
[20] T. Messay, R. C. Hardie and S. K. Rogers, "A new computationally efficient CAD system for pulmonary nodule detection in CT imagery", Medical Image Analysis, vol. 14, **(2010)**, pp. 390-406.